Energy Harvester Design for Intelligent Tyre Systems

Otso Jousimaa

School of Electrical Engineering

Thesis submitted for examination for the degree of Master of Science in Technology.
Espoo XX.XX.XXXX

Thesis supervisor:

Prof. Arto Visala

Thesis advisors:

M.Sc. Yi Xiong

D.Sc. (Tech.) Ari Tuononen

A " **Aalto-yliopisto**
Sähkötekniikan
korkeakoulu

Author: Otso Jousimaa

Title: Energy Harvester Design for Intelligent Tyre Systems

Date: XX.XX.XXXX   Language: English   Number of pages: 7+28

Department of Automation and Systems Technology

Professorship: Smart products

Supervisor: Prof. Arto Visala

Advisors: M.Sc. Yi Xiong, D.Sc. (Tech.) Ari Tuononen

Your abstract in English. Try to keep the abstract short; approximately 100 words should be enough. The abstract explains your research topic, the methods you have used, and the results you obtained. Your abstract in English. Try to keep the abstract short; approximately 100 words should be enough. The abstract explains your research topic, the methods you have used, and the results you obtained. Your abstract in English. Try to keep the abstract short; approximately 100 words should be enough. The abstract explains your research topic, the methods you have used, and the results you obtained. Your abstract in English. Try to keep the abstract short; approximately 100 words should be enough. The abstract explains your research topic, the methods you have used, and the results you obtained.

Keywords: For keywords choose concepts that are central to your thesis

Tekijä: Otso Jousimaa

Työn nimi: Energy Harvester Design for Intelligent Tire Systems

Päivämäärä: XX.XX.XXXX   Kieli: Englanti   Sivumäärä: 7+28

Automaatio- ja systeemitekniikan laitos

Professuuri: Älykkäät tuotteet

Työn valvoja: Prof. Arto Visala

Työn ohjaajat: DI Yi Xiong, TkT Ari Tuononen

Tiivistelmässä on lyhyt selvitys (noin 100 sanaa) kirjoituksen tärkeimmästä sisällöstä: mitä ja miten on tutkittu, sekä mitä tuloksia on saatu. Tiivistelmässä on lyhyt selvitys (noin 100 sanaa) kirjoituksen tärkeimmästä sisällöstä: mitä ja miten on tutkittu, sekä mitä tuloksia on saatu.

Tiivistelmässä on lyhyt selvitys (noin 100 sanaa) kirjoituksen tärkeimmästä sisällöstä: mitä ja miten on tutkittu, sekä mitä tuloksia on saatu. Tiivistelmässä on lyhyt selvitys (noin 100 sanaa) kirjoituksen tärkeimmästä sisällöstä: mitä ja miten on tutkittu, sekä mitä tuloksia on saatu. Tiivistelmässä on lyhyt selvitys (noin 100 sanaa) kirjoituksen tärkeimmästä sisällöstä: mitä ja miten on tutkittu, sekä mitä tuloksia on saatu.

Avainsanat: Vastus, Resistanssi, Lämpötila

Preface

I want to thank Professor Pirjo Professori and my instructor Olli Ohjaaja for their good and poor guidance.

Otaniemi, 16.1.2015

Eddie E. A. Engineer

Contents

Symbols and abbreviations

Symbols

$\mathbf{A}$	area
$\mathbf{B}$	magnetic flux density
c	speed of light in vacuum $\approx 3 \times 10^8$ [m/s]
ε	electromotive force
$\mathbf{F}$	mechanical force
$\mathbf{I}$	electrical current
$\mathbf{l}$	length
Φ_B	magnetic flux through loop area
ρ	resistivity
$\mathbf{P}$	power
$\mathbf{p}$	pressure
$\mathbf{U}$	input to system
$\mathbf{V}$	voltage
$\mathbf{Y}$	output from system
$\mathbf{Z}$	complex impedance

Operators

$\dfrac{\mathrm{d}}{\mathrm{d}t}$	derivative with respect to variable t
$\dfrac{\partial}{\partial t}$	partial derivative with respect to variable t
$\sum_i$	sum over index i

Abbreviations

AC	Alternating Current
BLE	Bluetooth Low Energy
DC	Direct Current
EMF	Electromotive Force
IC	Integrated Circuit
MEMS	Microelectromechanical Systems
MPPT	Maximum Power Point Tracking
PV	Photovoltaic
RF	Radio Frequency
SMPS	Switch-Mode Power Supply
TPMS	Tire Pressure Monitoring Sensors

1   Introduction

As technology advances, it has become possible to build small, light-weight and yet powerful sensor platforms which can communicate wirelessly with their environment. New kind of applications are being created using the possibilities given by these sensor platforms. A common feature with all of these devices is that they need power to function, even if the power needed is miniscule.

Traditionally wireless devices have been powered by batteries, but as the number of sensors increases, the cost of changing or charging batteries becomes significant part of cost of any system. This is especially relevant for the devices which are in hard-to-reach areas, such as inner parts of heavy machinery, walls of bridges and high rise buildings, remote environmental sensors et cetera. On some applications the life of the battery can become a limiting factor for the lifetime of entire system, as it's cheaper to replace the entire sensor with newer model than to keep using the old sensor with a new battery.

A new approach to powering the device is to harvest the energy from it's surroundings using ambient energy as the power source. Examples of such energy sources are solar, wind, temperature differentials, and vibration. The technology to utilise some of these power sources, such as wind and solar is already widely deployed and even used in the large-scale power production. On a smaller scale the demand for reliable and efficient solutions has been growing strongly with the advent of wireless low-power devices and a lot of research has focused on creating suitable technologies and devices for low-power energy harvesting.

This work focuses on powering one of such devices, namely a sensor inside a car tyre. The car tyre provides some unique challenges and opportunities, as there is a lot of energy available, but on the other hand operating conditions can be extremely harsh with large temperature ranges and extreme vibration and shocks especially in rougher road conditions.

Car tyre sensing itself has been in focus of a lot development lately, as legislation in the United States demands new tyres being fitted with a pressure sensor to warn drivers about the low pressure and related higher fuel consumption, wear on tyre and even elevated risk of accidents. European Union has also laws which require Tire Pressure Monitoring Sensors (TPMS) on new passenger cars.

Energy harvesting system is designed to provide enough power for the sensing of the critical parameters in tire, such as pressure, temperature and acceleration. This work provides a proof of concept of an energy harvester which is capable of supporting a radio link, microcontroller and a sensor.

Second section of this work details the background and previous work done on sensors of a tire. Third section presents the theoretical work and design of energy harvester as well as theoretical estimates for efficiency of system. Fourth section presents the experimental results from building the system. Conclusions are presented in the fifth section.

2 Background

2.1 Structure of a tyre

Tyres are composed of several layers with different functions. Figure 1 by Gent et al. [12] shows the layered structure. From outer tread to inner lining, the layers are:

Tread provides traction for driving, braking and cornering. Pattern and materials on tread is a compromise between wear resistance, traction, handling and rolling resistance

Belts provide mechanical strength, impact resistance and keep tyre from expanding under centrifugal forces.

Body ply provides strength to contain the air pressure.

Innerliner is a compound specifically designed to improve air retention in tyre.

In addition there are layers designed to improve tyre reliability, such as the belt wedge which reduces shear between belts.
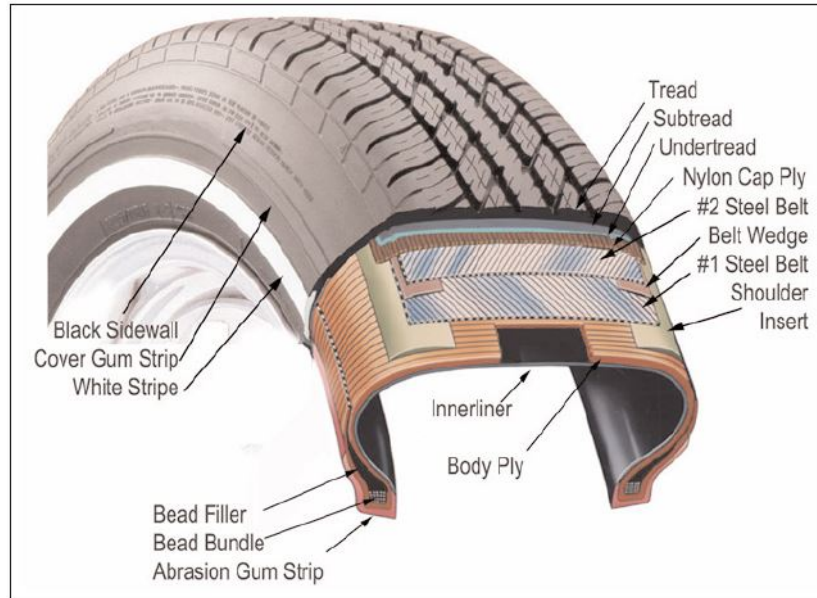

Figure 1: Structure of a tyre [12].

In endurance testing of tyres the car is driven at test track in three shifts, until desired number of course driving kilometers have been reached. In outdoor testing each company has their own proprietary test protocol. Indoor testing has standards, which mandates pressure, ambient temperature and speed as well as time driven. According to Gent et al. [12] this indoor testing takes 34 hours of driving at 120 km/h. 3 In addition to endurance testing, there is high-speed testing where tyre speed is gradually accelerated in steps of 10 km/h at regular intervals until target speed is reached.

2.2 Environment inside tyre

The energy harvester will be placed inside the tyre. Previous studies by Niskanen et al [23]. have shown that the tyre will experience acceleration in all three axes. Tangential and centripetal accelerations are dominant, they can reach amplitudes up to 150 g in test fixture. In addition a study done by Löhndorf et al. [19] shows shock survival of up to 4 000 - 5 000 g is required for reliability.

Temperature inside of the tire will reach equilliberium in ambient + 5-10 °C, so operation temperature should be in range of -40 to + 75 °C to have some safety margin on top of usual Finnish ambient conditions reasonable tempetature range?.

Previous work by Niskanen et al. [23] was used to as a basis for analysis of characteristics of acceleration inside the tyre. Raw data was used to gather minimum and maximum values of acceleration as well as frequency components inside tire. Data was gathered at 20 km/h, 60 km/h and 80 km/h speeds. Figures 3 and 4 are time domain representations of the acceleration along 3 axes as shown in figure 2.
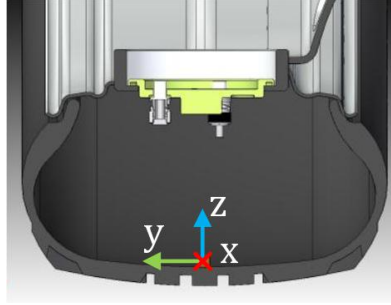

Figure 2: Axes in measurement by Matilainen et al. [20]

Frequency domain representations were calculated in Matlab. There are two main contributors to base frequencies: first is the rotational frequency of tyre itself and second is the impact when the tyre deforms as it contacts the drum.. There is clearly visible series of frequency components spaced at the rotational frequency of tyre as well as shock harmonics at upper frequencies. Figures 5 and 6 show the total frequency spectrum and the dominant frequency components. Images to be redrawn, labeled properly, font size increased, combined into one. Check the windowing..

It's important to notice that the sensor used was piezoelectric, which forms a highpass filter as the operation of sensor is based on charge between layers. This charge dissipates over time, so the steady-state centripetal acceleration reads as zero. Any device on the rotating tyre will experience centripetal acceleration (acceleration towrds centre of rotation) at the amplitude of:

$$a_{centripetal} = \omega^2 r, \tag{1}$$

where ω is the rotation speed of tyre and r is the radius of rotation.
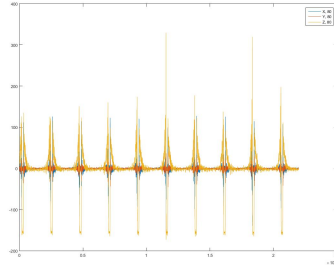
Figure 3: Acceleration of inner lining of tyre at 80 km/h in time domain.
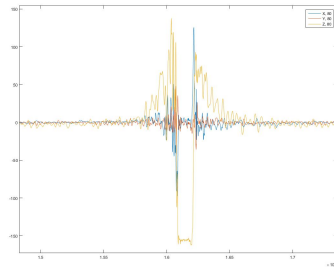
Figure 4: Acceleration of tyre inner lining in single rotation at 80 km/h.

2.3 Energy harvesting

2.3.1 Overview of methods

First step of designing a system for energy harvesting was to identify the currently known methods and their properties. Kubba et al. [16] have done a study on tyre pressure sensor technology, they present electromagnetic, electrostatic, piezoelectric and thermal solutions as possible candidates for energy harvesting. In addition, triboelectric and magnetostrictive methods have been proposed by Bowen et al [7]. Outside of the context of tyres, Paradiso et al. [25] present solar and radiowave

Figure 5: Frequency domain representation of acceleration data.

Figure 6: Most of the energy is found in 10-100 Hz range.

harvesting techniques. Radioactive power source has been suggested by Lal et al [17].

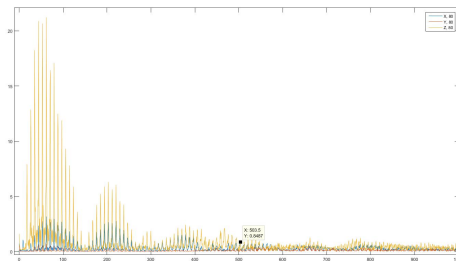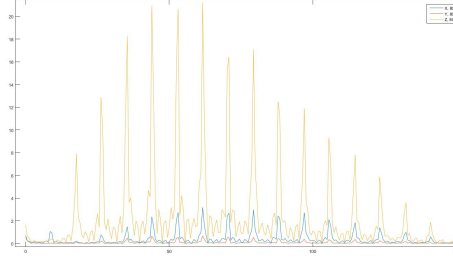Electromagnetic power sources are based on Faraday's law of electromagnetic induction. A magnet and a coil are put in motion relative to each other, and the changing magnetic flux through the coils of the generator produces voltage. Current through such device is determined by load resistance. Technology is widely used in power generation, where a primary power source such as wind or flow of water provides rotation for the generator. While conventional designs use rotational movement, linear generator designs exist. Boldea and Nasar [5] provide an overview of linear generator and actuator theory.

Electrostatic devices charge plates of a capacitor and use mechanical vibration to vary the structure of the capacitor. As the capacitance value changes with the structure, energy can be harvested from increased potential energy in capacitor. Drawback of this method is the required control electronics and high polarization voltages needed for maximal efficiency. There are also electrostatic methods which use electrets. These electrects hold constant charge and polarization for years and they can be used in electrostatic harvesters which do not require an external exitation source [4]. As electret elements and electrostatic generators are not readily available, they have been excluded from this study.

Piezoelectric materials generate charge in response of mechanical stress. This stress can be caused by firmly attaching the piezoelectric element to a surface which deforms (simply supported) or by leaving one end of the element free-hanging while other end is fixed (cantilevered). Dynamics of the generator are very different for the different configurations, Kim et al. [15] provides a model for impact-based piezoelectric harvester while Erturk et al. have done in-depth analysis of cantilevered piezoelectric modeling [8].

Thermal solutions can be further diveded into subcategories. Seeback-effect where a temperature gradient in a semiconductor material causes voltage between poles of the material is widely used in temperature sensing, but to generate appreciable amounts of power large temperature gradients of over hundred °C are required according to study by Amatya et al. [1]. Such temperature gradients are not practical inside the tyre. Pyroelectric materials do not require differential of temperature, they generate energy when the temperature of the entire element changes [33]. As the temperature inside tyre remains rather constant over long periods of time, these methods are not

practical for this application.

Triboelectricity generates power using friction between two materials, a classic example of this is Benjamin Franklin's experiments on charging various rods by rubbing them against different materials. A flexible triboelectric generator has been presented by Fan et al. [10]. Triboelectric sheets are not readily available and their construction is complex, so triboelectric generation is excluded from this work.

Magnetostrictive materials change their magnetic field in response to external mechanical sterss. This change can be utilised to create a magnetic flux through coils as in electromagnetic generators. A magnetostrictive generator was built by Wang et al. [31].

Solar energy can be harvested by using sun as a energy source for a thermal energy harvesting or by utilizing the photovoltaic (PV) effect to generate electricity from photons hitting PV material. PV technology is mature and widely used, and PV cells attached to rim of tyre could produce ample power during summertime. PV cells would however incur extra maintenance as the rims would have to be cleaned whenever power output falls.

Radio wave harvesting uses antennas to collect energy from ambient radio trans-missions, such as WiFi- and cellural signals. Patel et al [26] have built a demonstration device which uses TV broadcasts as an energy source. The tyre material dampens any Radio frequency (RF) broadcasts, which makes RF energy harvesting poorly suited for the application.

Radioactive energy harvesting resembles battery or fuel cell. A radioactive material is deposited in generator near piezoelectric cantilever. Radioactive decay charges proof mass of piezoelectric cantilever until the proof mass contacts the radioactive material by electrostatic attaraction, at which point the electrical charge is balanced and piezoelectric beam begins resonant vibration as in normal piezoelectric harvesting. Such a battery has lifetime limited only by half-life of the used material. Lal and Blanchard [17] present such a battery. This kind of battery would be redundant for the application, as there already exists energy in rotation of tyre which can be used to energise the cantilever.

In conclusion, a wide range of energy harvesting technologies have been identified. As their primary properties are known, we can narrow down the suitable technology to electromagnetic, piezoelectric and magnetostrictive. These technologies are studied further to identify optimal choice for the application.

2.3.2 Resonance-based piezoelectric harvesting

Piezoelectric materials produce voltage in response to mechanical stress. The effect is bidirectional, piezoelectric element can also produce mechanical strain in response to applied voltage. The material has crystalline structure with electrical dipoles in balanced state when no stress is applied. Mechanical stress unbalances these dipoles, creating element which resembles electronically a charged capacitor.

A common approach to piezoelectric harvesting is to configure the element as a cantilever and tune the resonant frequency of the system to dominant frequency of the surrounding environment. In some applications, such as in machines running

at the frequency of power grid (50 HZ or 60 HZ) this kind of frequency-tuning is relatively straightforward. TODO

2.3.3 Impact-based piezoelectric harvesting

As the resonant harvesting is not feasible in the environment inside tire, another method would be to use an impactor to hit a piezoelectric plate on every cycle of a tire. These impacts would provide energy once per rotation of a tire. This method has been tried before by Cite and it was found to provide up to 4 mW of power in average. TODO

2.3.4 Electromagnetical harvesting

Electromagnetical harvesting is based on Faraday's law of induction: A loop of wire acquires electromotive force (EMF) in response to a changing magnetic field. More formally:

$$\varepsilon = -\frac{d\Phi_B}{dt}, \tag{2}$$

where ε is the EMF, Φ_B is magnetic flux through loop area, and t is time. Negative sign signifies that emf opposes the change of magnetic flux. For a tightly wound coil of wire, the equation can be stated as:

$$\varepsilon = -N_{turns}\frac{d\Phi_B}{dt}, \tag{3}$$

where N_{turns} is the number of turns in a coil. [32, p.999]

It's important to notice that magnetic flux through wire Φ_B can change for a variety of reasons: the source of field can be in motion, strength of field can vary, the coil can be in motion, and the shape of coil can vary. In an energy harvesting application in an environment with vibrations motional energy is readily available, so we focus on energy harvesting methods which either move the source of magnetic field or the coil itself.

It can be determined from equation (3) that the energy available increases with the strength of magnetic source, number of turns in a coil and rate of change in the magnetic field.

Magnetic source can be either a permanent magnet or an electrically induced source as in induction motors. Induction-based generators require reactive power to start up, which means that any harvester design incorporating an induction generator would need a secondary power source to start the inductive generator. Hence the focus of this thesis will be in permanent magnet designs.

In addition to voltage available from the generator, it's important to consider the source impedance. A very simple electrical equivalent model of the generator is presented in figure 7, where generator is presented as a voltage source in series with lumped inductor and resistor [14].

This model is greatly simplified and it does not account for factors such as effect of electromagnetical force on mechanical structure of the generator. Even with these

Figure 7: A simple electromachanical generator equivalent circuit.

.

limitations, the model is still useful as it can be used to determine an optimal load for the generator.

The power output can be written formally as:

$$P_{generated}(s) = \varepsilon(s) * I_{generated}(s), \tag{4}$$

where $P_{generated}(s), \varepsilon(s), I_{generated}(s)$ are complex frequency-domain power, voltage and current dependent. Voltage is determined by EMF as described above. Current can be written as:

$$I_{generated}(s) = \frac{\varepsilon(s)}{Z_{generator}(s) + Z_{load}(s)}, \tag{5}$$

where $Z_{generator}(s)$ and $Z_{load}(s)$ are complex impedances of load and generator. This equation is valid only for linear systems, so for example rectifying and converting power with switch-mode power supply (SMPS) reduces accuracy of the equation. Substituting (5) into (4) we obtain:

$$P_{generated}(s) = \varepsilon(s) * \frac{\varepsilon(s)}{Z_{generator}(s) + Z_{load}(s)}. \tag{6}$$

Total power into load can be written as:

$$P_{load}(s) = \varepsilon(s) * \frac{Z_{load}(s)}{Z_{generator}(s) + Z_{load}(s)} * \frac{\varepsilon(s)}{Z_{generator}(s) + Z_{load}(s)}. \tag{7}$$

It's easy to see from (7) that if the load impedance is infinite or zero, there is no power generated. It can be shown that maximum power is generated when load impedance is complex conjugate of generator impedance, $Z_{generator}(s) = Z_{load}(s)^*$. Another consideration is efficiency of the generator: the electrical efficiency is defined as ratio of power flowing into load and total power generated. Equation (7) can be used to show that when load impedance is equal to generator impedance, efficiency is 50%. Efficiency rises with the load impedance, which is why generators are rarely run at their maximum power. In our application the harvested power is minuscule compared to power available in tire, so it makes sense to try to match the load impedance for maximum power.

In an energy harvesting application it is important to consider the validity of established theory when generator is scaled to centimetres or even smaller dimensions. Many assumptions, such as coil being tightly wound and made of thin wire might

become invalid at microscale. O'Donnel et al. [24] have done a study on the effects of scaling dimensions downwards down to millimetre range, and they concluded that power available from generator is proportional to fourth power of generator dimension for cubical generators. Another of their primary findings was that a microfabricated generator becomes more effective than a traditional wire-wound generator when design is scaled below $2mm$ length or in $8mm^3$ volume. It can be concluded that in this application it is reasonable to use a wire-wound generator over microfabricated one, as the generator dimensions can be an order of magnitude larger than this crossover point.

2.3.5 Magnetostrictive harvesting

TODO: Magnetostrictive harvesting resembles piezoelectric harvesting. Figure 8 shows proposed system, where magnetostrictive cantilever is sandwiched between biasing magnets and a pickup coil.
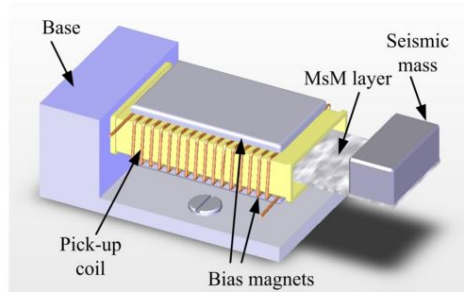

Figure 8: A magnetostrictive energy harvester by Wang et al. [31]

.

3 Design

3.1 System-level design

The complete system will consist of energy harvesting source, energy storage for times when harvested energy is not available, AC/DC and DC/DC converters for maintaining required voltage levels in different blocks of system, accelerometer for measuring the accleration in tyre and radio/microcontroller module for transmitting data from acceleromoter. Figure 9 shows the power and data flow between subsections of system.
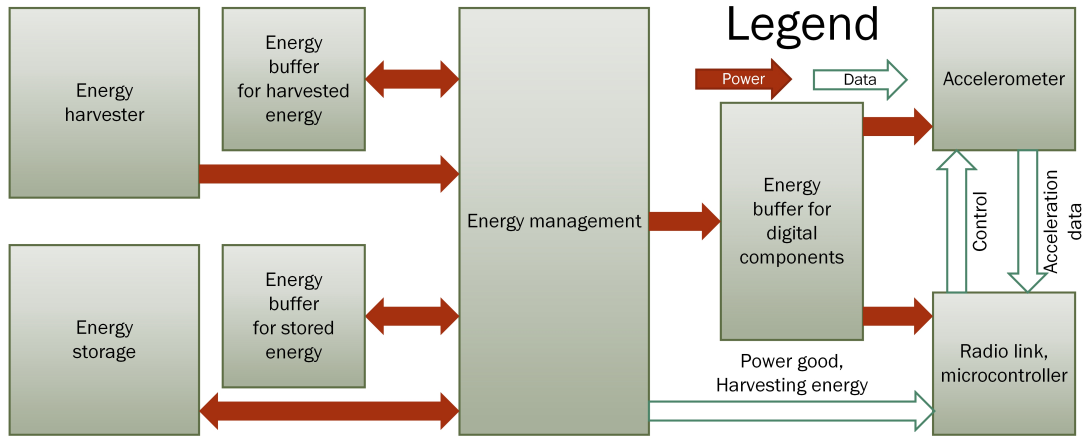

Figure 9: Block diagram of complete system.

3.2 Power requirements of a system

The sensor system will be in three distinct states. One is sleeping, conserving power as much as possible while car is not moving. Second state is measuring, when the radio connection is off but electronics are active and gathering data. Third state is transmitting, when the data is relayed to drive computer in car.

Energy and power consumption are estimated by reviewing a few suitable components and their power requirements. Energy management is handled by a specialized integrated circuit (IC), for example LTC3331 [29].

Communication is handled by a Bluetooth-low energy (BLE) module, which contains a general-purpose microcontroller for application flow control. We use BLE113 [3] as an example of such module.

Finally there is an accelerometer which is used for gathering data out of the system, ADXL375 [28] is used as an example. ADXL is a low-power digital accelerometer with dynamic range of 200g. Table 1 summarizes the estimated power requirement of each subsection of system. System level voltage is selected to be 2.5 V, as that is lowest voltage which LTC3331 can supply and allows all devices to function. Lowest possible voltage is selected to reduce the power draw.

Table 1: Current and power consumption of system at different activity levels.

Device	Sleep	Monitoring	Communicating
LTC3331	0.2 μA	80 μA	16 250 μA
BLE113	0.9 μA	275 μA	26 000 μA
ADXL375	0.1 μA	140 μA	140 μA
Total power	3 μW	1 200 μW	110 000 μW

Power consumption grows by orders of magnitude when the activity is stepped up to the next level. Therefore it's important to keep the system in sleep whenever possible, for example when the car is parked and wake up only periodically to check if movement has started. Monitoring starts once car is moving, and device will send brief pulses over the radio link when necessary.

Battery manager power draw is estimated by calculating required power to supply the rest of the circuit at 80 % efficiency.

3.3   Electromagnetical harvester design

3.3.1   Basics of electromagnetical vibration harvester

Electromagnetic harvesters utilise vibration to move a magnet inside a coil. The movement of a magnet causes a changing magnetic field, which gets coupled to a coil. The coil opposes the change in magnetic field by inducing electrical current in the device. A device could be built with a spring-loaded magnet to balance out the static acceleration of a tyre, an added benefit to spring loaded mechanism would be the utilisation of resonant frequency of the spring-mass system: as the system gets a shock, some of the energy would be in correct frequency range to make the magnet oscillate inside coil allowing generation of energy until next shock. The coil will also function as a damper to system, so no extra damping is required. Modern neodymium magnets do not lose their magnetization by vibration, so long magnet can be reliable for a long time period.

A theoretical design of linear generator (LG) was made. Most common generator designs use a rotating magnet inside coils to generate alternating current. As the mechanical apparatus for converting the linear accelerations inside the tyre to rotational movement would add to complexity and cost of the tyre, generator is designed to use the linear motion as the power source.

Basic principle of operation of LG is similar to traditional rotational generator. A moving magnet creates alternating magnetic field which is coupled to coiled conductors. The conductors oppose this change of magnetic field by inducing an electrical current across their ends. The design can have multiple phases and poles, where phases refer to parallelly connected coils and poles refer to serially connected coils. Multiple phase designs can have lower resistive losses in wiring, as the resistive losses are propotional to square of the current. However paralleling phases requires

separate rectification for each phase, which leads to increased rectification losses. Adding poles to design increases the output voltage and frequency, but having a small airgap between the coils and magnets becomes critical to maintain efficiency of the generatorcite a study of multi-pole.

Energy harvester designs sometimes use several poles to increase the frequency of the power output cite. This increased frequency allows to use smaller energy storage components such as capacitors to keep the device powered until next cycle. The characteristics of the tyre make this point irrelevant, as energy is available once per revolution of the tire when generator contacts the ground and when the contact ends. Any energy storage device has to maintain power until the next cycle, and no increase of the frequency while generator is in contact can alleviate that. Therefore number of poles is minimized to reduce complexity. Pole number is selected as two, so there is one negative and one positive pole. Mechanical design can utilise resonant vibration to function as energy storage device instead of electrical or electronic storage.

First design decision was whether to use a moving magnet or moving coil type of a design. Moving coil designs tend to have lighter moving parts which is a very important feature in high-power designs where mass of the generator is large. On the other hand, moving coil require flying leads cite development of a moving magnet linear. which is a long-term reliability concern cite linear electric actuators and generators. cite book Boldea, Nasar Linear electric actuators and generators p 203. conclude that moving coil designs aren't practically interesting, so the design is focused on moving magnet generator.

A rough model for designing initial prototypes was done previously by cite backpack harvester. As the work verified the model experimentally and found the model to be reasonably accurate, it was adapted to form basis of linear generator model. The model can account for most of the key design parameters.

There are two different approaches to generator structure. One is magnets inside, and coils on the outer rim of the generator. Other is to use ring magnets on the outer rim and have the coils on the inside. Both methods have their advantages: Having magnets on the outside allows larger and therefore stronger magnets and creates horizontal support for the magnets as they slide along the shaft. Having coils on the outside increases wiring radius which results in greater power if other parameters are held equal. In-depth study of both concepts is done to select optimal structure for generator.

The height of the generator is constrained at confirm 45 mm. Initially the height of the generator was selected to be 35-40 mm to leave some margin while still being as tall as possible. Lower weight is desirable to avoid unbalancing the tyre, but there is no specific absolute maximum mass for the device.

A method to counter the centripetal acceleration is needed to keep the magnet on the centre of the generator. Ideally, such method would always balance the magnet in the middle of generator against any external constant force, but active control is not achievable without adding to complexity and power consumption of the generator itself. Passive negative feedback method has to be used instead.

Springs are often chosen cite few sources to balance the magnets, but as the centripetal acceleration grows exponentially with the speed of the car, any linear

spring would be usable only for very limited range of speeds. Non-linear conical springs which have the added benefit of compressing into very small height are available.

Another approach would be to use two additional magnets fixed to top and bottom of the generator in repulsive configuration. Force between magnets is inversely propotional to fourth power of the distance [2], which leads to a strong negative feedback on the position of the magnet. Tornincasa et al. [30] proposed one such design, shown in figure 10.
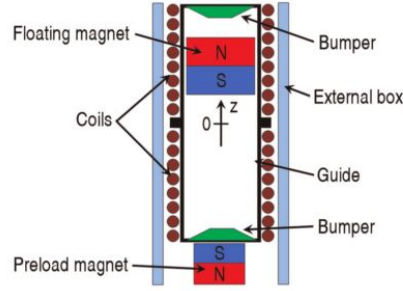

Figure 10: A magnetically balanced linear generator by Tornincasa et al. [30]
.

Magnetic floating is an attaractive solution, as magnets can be thin and they do not wear out with aging. On the other hand, any imbalance in the magnets result in torgue which causes increased friction. picture? This issue is further aggravated in designs where shape of the generator shaft is not a smooth cylinder. Therefore the design should have any grooves filled with suitable epoxy and the shaft should be sanded or turned to final diameter to ensure smooth sliding of the magnet across the length of the shaft.

3.3.2   Analytical model of electromagnetical vibration harvester

A common starting point for analysis of linear generator is to model the mechanical domain as Mass-Spring-Dampener system decipted in figure 11. A mass "floats" in system, a spring balances the mass towards centre and a damper represents frictional forces opposing any movement of mass.

Input Y is the force applied to the base of system, output U is the position of mass block relative to "zero". Zero is usually set to point where mass settles when no input, including gravity, is applied to system. Paramters m, D, and k are mass, damping constant and spring constant of system, respectively. Input-output-equation in time domain can be written as:

$$m * \ddot{U}(t) + D * \dot{U}(t) + k * U(t) = Y(t). \tag{8}$$

As the force $Y(t)$ is defined as $Y(t) = m * a(t)$, and the acceleration $a(t)$ can be considered constant regardless of any reasonable mass m of system, equation (8) can be written as:
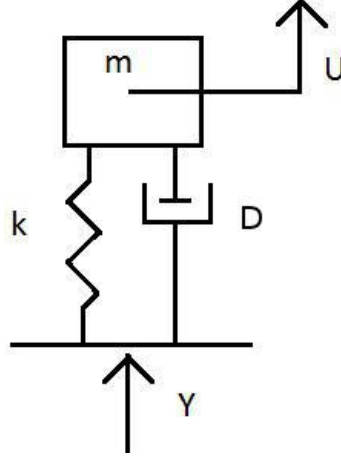
Figure 11: Mass-spring-damper system.

$$\ddot{U}(t) + \frac{D * \dot{U}(t)}{m} + \frac{k * U(t)}{m} = a(t). \tag{9}$$

This form is convenient for analysis, as the acceleration measurements from previous research are available and they represent real-world values. Mass m can be considered constant, as the system does not exchange matter with surrounding environment. As magnetic suspension was selected, the paramter k cannot be considered as a constant, but rather a function of mass position $k(U)$. Centripetal force can be considered as a constant DC-component of function $Y(t)$, and is not included in analysis of function $k(U)$. According to D. Amrani [2] force between two magnets can be approximated as

$$F(x) = \frac{3\mu_0 m_1 m_2}{2\pi} * \frac{1}{x^4}, \tag{10}$$

where $F(x)$ is force as a function of distance x between magnets, μ_0 is the permeability of vacuum, m_1 and m_2 are magnetic dipole moments of magnets under examination. This equation is only valid when x » h, where h is thickness of the magnet. As two magnets are used to suspend the rotor magnet, total force acting on mass becomes

$$F(x) = \frac{3\mu_0 m_r m_l}{2\pi} * \frac{1}{(x_0 + x)^4} - \frac{3\mu_0 m_r m_u}{2\pi} * \frac{1}{(x_0 - x)^4}, \tag{11}$$

where m_l, m_u, m_r are magnetic dipole moments of lower suspending magnet, upper suspending magnet, and rotor magnet. x_0 is the distance to middle point of generator and x is the displacement of rotor magnet from aforementioned middle point, positive direction being upwards. Figure draw figure shows the system.

Regrettably, the expression (11) is very inaccurate for magnets where diameter is large compared to thickness of magnet, and the problems are compounded when distance between magnets is small. Therefore final design should be optimized using measurement data or finite element analysis (FEA) for determining $k(U)$.

Damping parameter D is likevise a function electromagnetic force acting on magnet, friction between magnet and stator and pneumatic damping caused by compression of air in generator. Tornincasa et al. [30] divided this damping parameter into three distinct terms to account for these different physical phenomena in damping. Let us call them $D_{emf}, D_{friction}$, and D_{air}, respectively. D_{emf} represents power extracted from the system into electrical current, it can be written as:

$$D_{emf} = BIlsin(\phi), \tag{12}$$

where B is magnetic field affecting coil (presumed constant), I is current through wire depending on load and generator properties, l is total length of wire in coil and ϕ is angle between coil and magnetic field, presumed to be 90 °. Assuming the load impedance is the complex conjugate of coil impedance for maximum power harvesting, we can substitute the I with equations (3) and (5), which results in:

$$D_{emf} = B\frac{\varepsilon}{2 * Re(Z_{generator})}lsin(90°), \tag{13}$$

where $Z_{generator}$ is the impedance of generator. As the load impedance is complex conjugate of generator impedance, their series connection has only real (purely resistive) component. This assumption fails on real-world application with non-linear rectification and DC/DC conversion, but it can be used as a basis for analytical examination of the generator. As ε can be substituted with (3), we obtain:

$$D_{emf} = B\frac{-N\frac{d\Phi_B}{dt}}{2 * Re(Z_{generator})}lsin(90°), \tag{14}$$

The relationship between $N\Phi_B$ and $Re(Z_{generator})$ can be further studied by writing

$$\Phi_B = \iint_{\Sigma(t)} B(r,t) \, dA, \tag{15}$$

where $\iint_{\Sigma(t)}$ signifies possibility of loop area changing over time and dA is element of surface area. If we assume the coil to be a perfect tightly wound circle which does not deform over time, we can write the relationship between number of turns in coil, area of coil, and resistance of coil as:

$$R = N2\pi A\rho_{wire}, \tag{16}$$

where ρ_{wire} is resistivity of coil wire. Substituting (16) and (15) into (14) we finally obtain reasonably accurate expression for D_{emf} which accounts for all the design parameters affecting it:

$$D_{emf} = B\frac{-N\frac{d[\iint B(r,t) \, dA]}{dt}}{2 * N2\pi A\rho_{wire}}lsin(90°). \tag{17}$$

A few observations can be made from this equation: first, the magnetic field strength B and it's derivate in respect to time increase the D_{emf} which signifies the

electrically extracted useful power. Therefore it makes sense to use as strong magnets as possible, as long as other parameters aren't adversely affected. Second, both the number of turns and the loop area are as multipliers and divisors, which means they should be optimized to find best applicable values. Third, resistivity of wire limits power that can be extracted, so intuition would lead to minimizing wire resistance. In practise the wire resistivity can be decreased by increasing wire diameter, which in turn leads to lesser number of turns in same volume and mass of coil. Therefore, also wire diameter and material should be optimized to find desirable compromise in generator design.

Next we examine $D_{friction}$ in detail. Friction is modelled as Couloumb fricion:

$$F_s = \mu_s N, F_k = \mu_k N, \tag{18}$$

where F_s and F_k are static and kinetic friction forces opposing movement, μ_s and μ_k are friction coefficients in static and kinetic situations and N is normal force along X- or Y- axis. Normal forces are estimated by using existing acceleration data and calculated mass of magnet. Coefficients of friction are looked up from supplier of stator material. Transfer between static and kinetic models is assumed to be a step, if velocity of magnet is 0 along Z-axis, μ_s is used, μ_k othervise.

Finally, there is pneumatic damping of the system, D_{air}. In a closed tube, the central magnet can be thought as a piston dividing generator into two chambers. If there is insignificant airflow between chambers, any force caused by pressure deltas between chambers act as a spring. However, some airflow is to be expected due to clearance between magnet and stator. Tornincasa et al. [30] modelled this effect by adding a virtual centrepoint for pneumatic spring, this centre moves through a virtual damper which models the airflow between chambers. End result is that pneumatic spring takes some energy from movement, and this energy stored into pneumatic spring is dissipated as the centre moves until potential energy stored in the spring is zero.

The force from pressure differential is:

$$F_{\delta p} = \frac{\pi d^2}{4}(p_{lower} - p_{upper}), \tag{19}$$

where d is diameter of magnet and $p_{lower} - p_{upper}$ are pressures in chambers. Pressures can be estimated from ideal gas law:

$$pV = NRT \tag{20}$$

where p is pressure, V is volume, N is amount, R is ideal gas constant and T is temperature. Temperature is assumed to be constant. Initial pressure is assumed to be same as tyre pressure and magnet is assumed to be exactly in midpoint at start. Change of volume can be calculated from change of height caused by movement of the magnet.

Mass flow between sections can be estimated with equation given by Fox et al. [11]:

$$\dot{m}_{1\rightarrow2} = \frac{\rho\pi d\delta_{r^3}}{12\mu h}(p_1 - p_2), \tag{21}$$

where ρ is air density, δ_r is radial clearance, μ is dynamic viscosity and h is the height of magnet. [30]

There is also frictional dissipative force as the air passes along the edges of the cylinder. This frictional force has magnitude of:

$$F = \mu * \rho * \frac{\pi dh\dot{z}}{\delta}[21]. \tag{22}$$

Analytical expressions for the equations governing the mechanical movement of magnet inside generator have now been identified. Some of the non-linear functions are hard to solve analytically, therefore experimental or FEA methods should be used for creating approximations for these functions.

The analytical effect of these parameters is summarized in table 2

Table 2: Effect of parameters of generator

Parameter	Increasing	Decreasing
N_{turns}	Higher voltage	Smaller size, less wiring resistance
N_{pole}	Increased frequency	Decreased frequency
l_{pole}	More space for wiring	Higher voltage, smaller size
A_{loop}	More power	Smaller length of wiring
B	Increased power	Smaller magnets
r_{wire}	Decreased wiring resistance	More turns in same space
δ_r	Stronger side walls	Incresed efficiency

3.3.3 Experimental and FEA modeling of electromagnetic harvester

As some parameters of the harvester are difficult to solve analytically, these parameters are solved using experimental and FEA methods. First one of these difficult interactions is the magnetic force between rotor magnet and balancing magnets. A magnetics FEA software FEMM [22] was used to create an axisymmetric model of magnets in generator. Figure 12 shows the used model. Model has two biasing magnets made of N40-neodymium alloy configured to repel an identical rotor magnet. Magnets have height of 2.5 mm and diameter of 11 mm, walls of generator are modelled as air. Generator has total height of 25 mm, leaving rotor magnet 17.5 mm room for movement inside generator.

Weighted stress tensor integration over rotor magnet volume as implemented by FEMM was used to determine FEA value for net magnetic force acting on rotor magnet. A LUA script was used to move the rotor magnet from bottom of the generator to top in 0.1 mm increments and values obtained from analysis were
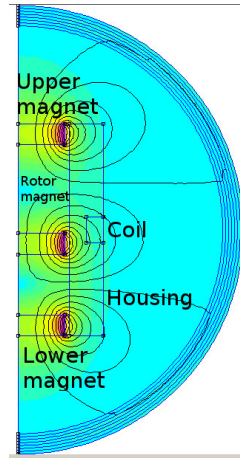
Figure 12: FEM model of generator magnetics

exported as CSV data for plotting in a spreadsheet software as well as to create a lookup-table for MATLAB/SIMULINK simulation. Figure 13 shows the force on magnet, positive force meaning force towards the upper magnet and zero height being at the bottom of cylinder. For reference the centrifugal force acting on magnet was also calculated at various speeds, assuming weight of the magnet is 1,67 g and radius to bottom of generator is 275 mm.
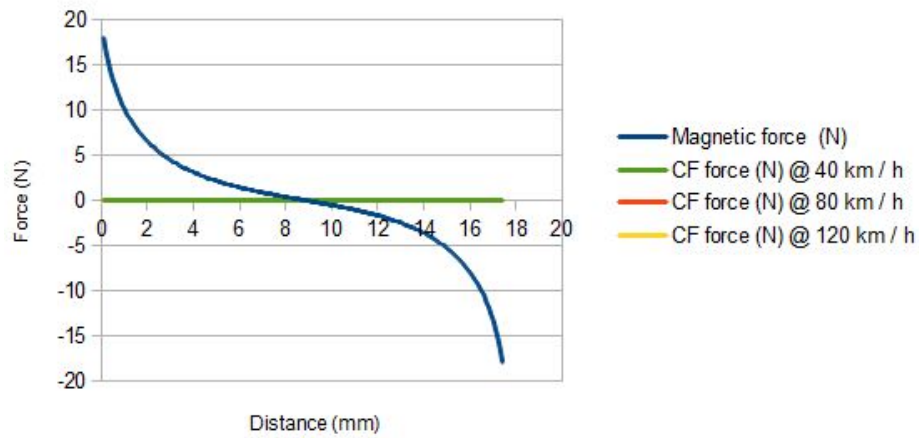

Figure 13: Forces acting on magnet

It can be seen that net force on rotor magnet is dominated by the magnetic forces. while centrifugal force on magnet is negligible in comparison.

Second use for this FEA analysis is to create look-up table for flux linkage into coils of generator. The methodology was similar to determining forces affecting the rotor magnet: a LUA script was ran to sweep possible magnet positions, and look-up table of flux linkage into coils was created. For the purposes of analysis, difference of flux linkage was calculated between each point. The change of flux linkage is a very

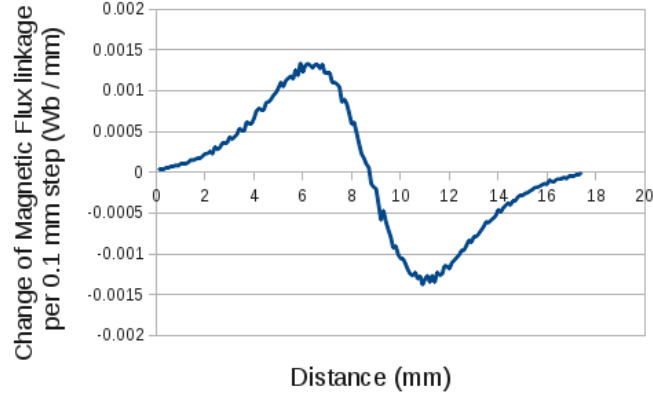important parameter, as the power generated is proportional to $\frac{d\Phi_B}{dt}$.

Figure 14: Flux linkage and rate of change in 0.1 mm steps in generator.

Based on these results, a magnet moving at the speed of $0.1mm/s$ would induce voltage of up to $1.5mV$ in each winding of the coil. If we assume coil to have 100 turns, travel length of the magnet to be 1 mm, and frequency of magnet moving inside generator to be 10 Hz the peak voltage out of generator would be sufficient to power the circuitry and charge battery of sensor.

3.4 Piezoelectric harvester design

A previous work by

3.5 Hybrid harvester design

3.6 Electronic design

3.6.1 Simulation of circuit

The analog sections of circuit were simulated using LTSpice IV [18]. Microcontroller, radiolink and accelerometer were simulated as resistive load. Battery was modelled as a voltage source with high-value capacitor and low-value resistor in series. Piezoelectric harvesting was modelled both as high-voltage source with capacitor in series and current source with capacitor in parallel. Electromagnetic harvesting was modelled as low-impedance low-voltage source.

once lookup-tables can be generated, create maximum power point tracking. LTC3331 presents an interesting opportunity for maximum power point tracking (MPPT). While the impedances of individual components cannot be tuned in real-time, the microcontroller can determine rotation frequency of tyre from accelerometer readings and determine the maximum power point. LTC3331 can adjust the target voltage for energy storage buffer capacitor, which enables MPPT-control of system.

The simulation model is shown in figure 15. Connections were adjusted as needed to generate simulation data for different purposes, such measuring energy efficiency, transient response, MPPT etc.
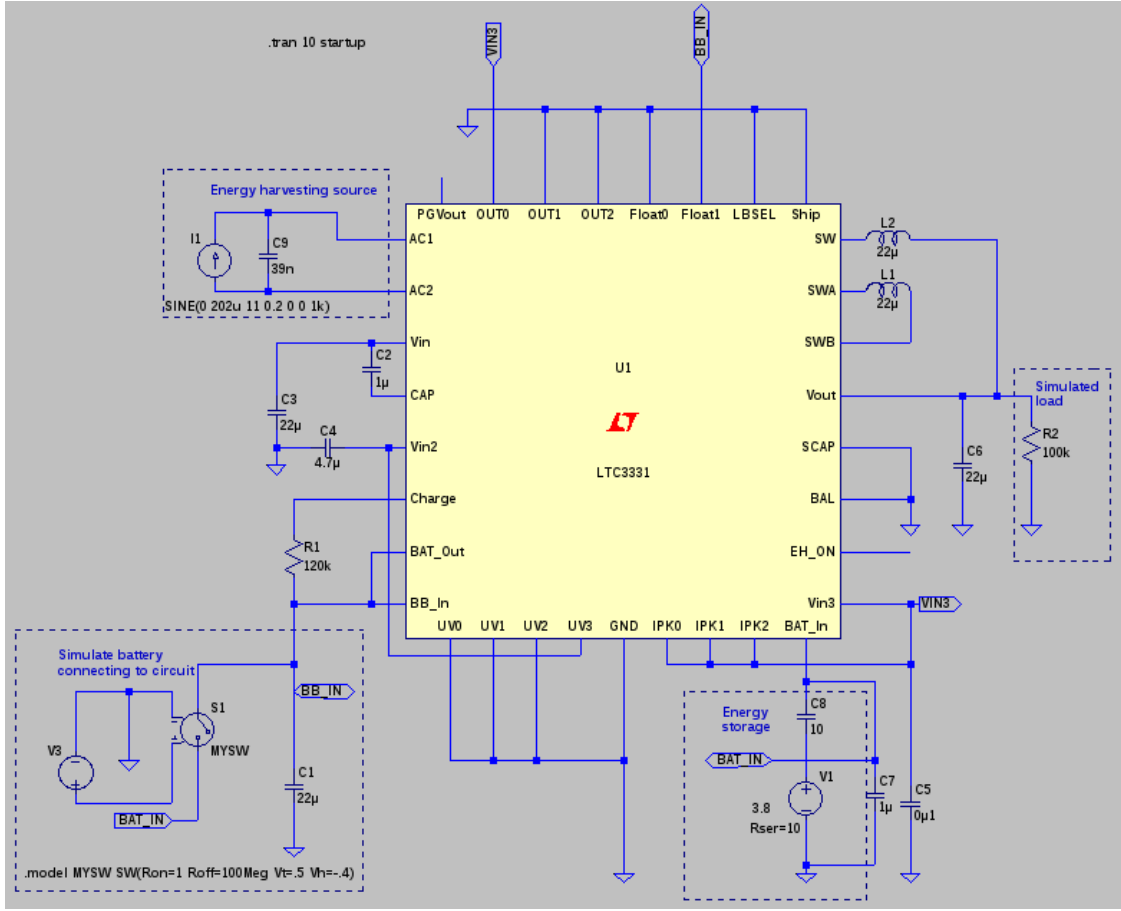

Figure 15: LTSpice [18] simulation of electrical circuit

–simulated efficiency –simulated mppt –figures

3.6.2   Schematic design

The printed circuit board (PCB) schematic is a logical representation of the components and how they connect to each other. The schematic is designed in accordance to datasheets, reference designs and application notes of main circuit components. As the design operates in high-vibration environment with wide temperature variations, special care is used to select components which have well-defined temperature and mechanical characteristics.

As the circuit is a low-power design, careful attention has to be paid to parasitic properties and non-ideal behaviour of components. For example electrolytic capacitor can have leakage current of several microamperes [6], which is in the same order
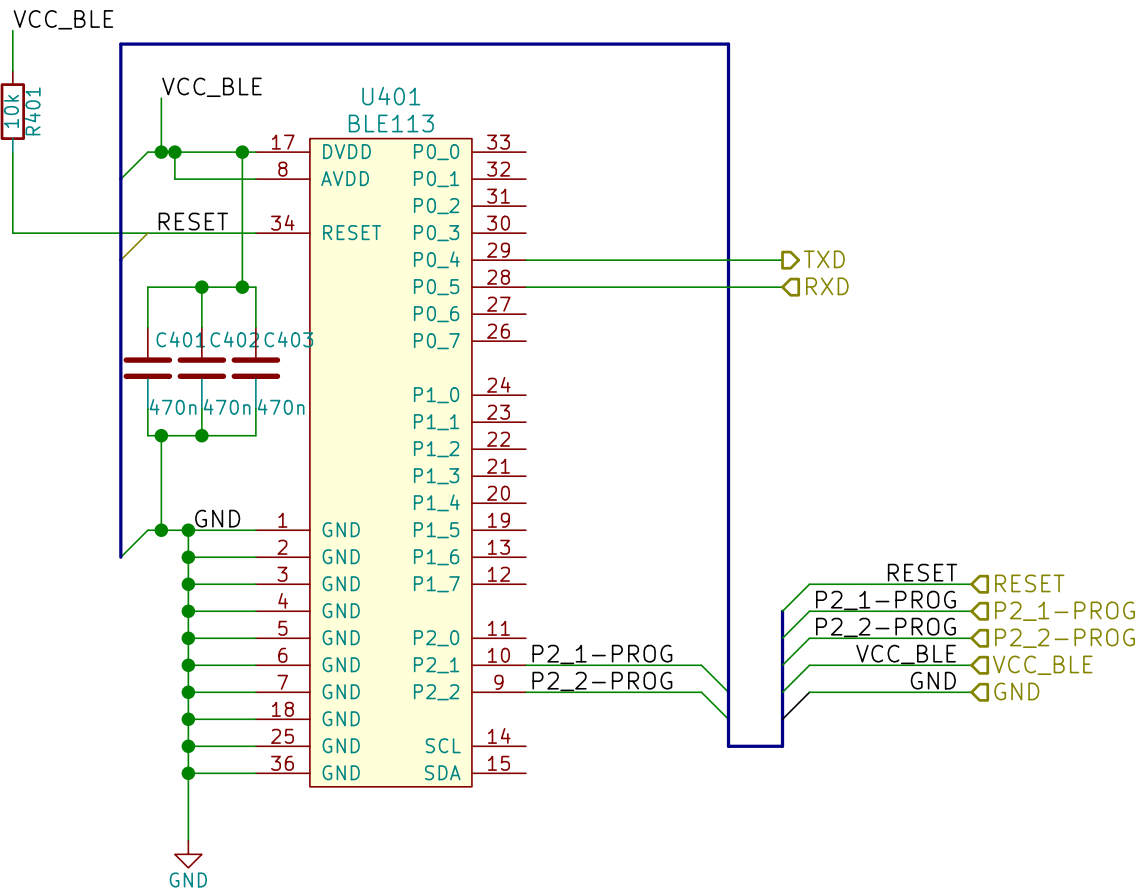
of magnitude as the targeted sleep current consumption of system. Likewise any signaling current should be kept at minimum.

Another important point of view is the modularity and testability of the circuit. All critical lines have provision for testing and debugging for development and verification of circuit functionality.

Power supply has some conflicting requirements, as any noise in power degrades radio and measurement performance, but on the other hand the power supply should be efficient switch mode power supply to keep power consumption at minimum. LTC3331 has switch-mode power supplies which can be used to generate supply rails for the rest of circuit, these are used and noise is dealt with by passive filtering.

Most of the power supply design is relatively straightforward application of ideas presented in LTC3331 datasheet, but a few special considerations have been given to minimize sleep power consumption. First of all, the configuration pins need to be controllable to enable MPPT. Any leakage current has to be minimized, and control is not needed while energy is not harvested.

3.6.3 Circuit layout

The PCB layout defines the physical placement of the components on the circuit board. Special care must be used in placement of accelerometer to measure vibration of tyre itself rather than resonances of PCB. Components have to be placed in a

manner which minimizes effect of vibrations on them.

3.7 Mechanical design

Material for the shaft has a few requirements. It has to have at least as good temperature characteristics as the magnet being used and it must be hard enough to not deform under impacts. Low friction coefficient is desirable as this leads to smaller losses, and long time durability under wear is of course desired. Being lightweight and easily machinable are also desired characteristics. As the generator is small, volumetric cost of the material is of little concern. For the electro-magnetic generator design material ferromagnetism has to be considered. Table 3 has comparison of different materials considered for the application.

Table 3: Materials for the shaft of generator [27], [9].

Material	Hardness	Friction	Durability	Temperature
PTFE(Teflon)	Very low	Lowest	Lowest	-190... + 250 °C
Polycarbonate	Very high	High [13]	-	-60... + 125 °C
PA 6 (Nylon)	Low	Medium	High	-40... + 80 °C
Oil-infused Nylon	Low	Very low	Very high	-20... + 105 °C
Acryllic	High	-	-	-40... + 70 °C
Polyacetal (POM C)	Medium	Low	Low	-50... + 105 °C

4 Results

4.1 Validation of harvester electrical model

A Simulink model was built to verify feasibility of the linear generator. The simulation included real acceleration data from previous studies made by cite and a model of generator as well as a simplified capacitive-resistive load. There is an abundance of previous work done on simulating linear generators cite, however a simplified model was used at this stage to get a proof-of-concept level generator. Further work remains in optimizing the design in terms of size, mass, power output, usable speed range, cost and long-term reliability.

4.2 Validation of harvester mechanical model

Text on estimating and measuring mechanical friction and strength of device.

4.3 Electrical performance of circuit

Text on measured electrical parameters, current and power consumption, timings, power supply efficiency etc.

4.4 System-level performance

Text on integration, testing inside tyre and test drive on real road.

5   Conclusions

References

[1] R. Amatya and R. J. Ram. Solar thermoelectric generator for micropower applications. *Journal of Electronic Materials*, 39(9):1735–1740, 2010.

[2] Djilali Amrani. Determination of Magnetic Dipole Moment of Permanent Disc Magnet with Two Different Methods. 2015.

[3] Bluegiga. BLE113 data sheet (v1.2). (November), 2013.

[4] S Boisseau, G Despesse, and B Ahmed Seddik. Electrostatic Conversion for Vibration Energy Harvesting. *Small-Scale Energy Harvesting*, pages 1–39, 2012.

[5] I. Boldea and S. a. Nasar. Linear electric actuators and generators. *IEEE Transactions on Energy Conversion*, 14(3):712–717, 1999.

[6] Jens Both. Leakage current properties of modern electrolytic capacitors.pdf. Technical report, 2001.

[7] C. R. Bowen and M. H. Arafa. Energy Harvesting Technologies for Tire Pressure Monitoring Systems. *Advanced Energy Materials*, pages n/a–n/a, 2014.

[8] Alper Erturk, Daniel J Inman, Scott L Hendricks, Michael W Hyer, and Ishwar K Puri. Electromechanical Modeling of Piezoelectric Energy Harvesters. *Health San Francisco*, 2009.

[9] ETRA. TEKNISET MUOVIT, 2015.

[10] Feng Ru Fan, Zhong Qun Tian, and Zhong Lin Wang. Flexible triboelectric generator. *Nano Energy*, 1(2):328–334, 2012.

[11] R W Fox, A T McDonald, and P J Pritchard. *Introduction to Fluid Mechanics*. 2008.

[12] a N Gent and J D Walter. The Pneumatic Tire. *Rubber World*, (February):707, 2005.

[13] Goodfellow. Polycarbonate (PC).

[14] Panida Jirutitijaroen. EE2022 Electrical Energy Systems Lecture 10 : Electric Power Generation – an Equivalent Circuit of a Generator. 2012.

[15] S H Kim, S Ju, C H Ji, and S J Lee. Equivalent circuit model of an impact-based piezoelectric energy harvester. *Journal of Physics: Conference Series*, 557:012094, 2014.

[16] Ali E. Kubba and Kyle Jiang. A comprehensive study on technologies of tyre monitoring systems and possible energy solutions. *Sensors (Switzerland)*, 14(6):10306–10345, 2014.

[17] B Y Amit Lal and James Blanchard. The daintiest of dynamos. *IEEE Spectrum*, (September):36–41, 2004.

[18] Linear Technology. LTSpice IV.

[19] M Löhndorf, T Kvisterø y, E. Westby, and E Halvorsen. Evaluation of Energy Harvesting Concepts for Tire Pressure Monitoring Systems. *International Workshops on Micro and Nanotechnology for Power Generation and Energy Conversion Applications*, pages 331–334, 2007.

[20] Mika J Matilainen and Ari Juhani Tuononen. Intelligent Tire to Measure Contact Length in Dry Asphalt and Wet Concrete Conditions. *Avec 12*, pages 1–6, 2012.

[21] Medhat K Bahr Khalil. Estimated versus Calculated Viscous Friction Coefficient in Spool Valve Modeling. pages 1–9, 2008.

[22] David Meeker. Finite Element Method Magnetics, Version 4.2, 2013.

[23] Arto J. Niskanen and Ari J. Tuononen. Three 3-axis accelerometers fixed inside the tyre for studying contact patch deformations in wet conditions. *Vehicle System Dynamics*, 52(sup1):287–298, 2014.

[24] T O'Donnell, Chitta Saha, Steve Beeby, and John Tudor. Scaling effects for electromagnetic vibrational power generators. *Microsystem Technologies*, (April):26–28, 2007.

[25] Joseph a. Paradiso and Thad Starner. Energy scavenging for mobile and wireless electronics. *IEEE Pervasive Computing*, 4(1):18–27, 2005.

[26] Deep Patel, Rohan Mehta, Rhythm Patwa, Sahil Thapar, and Shivani Chopra. RF Energy Harvesting. *International Journal of Engineering Trends and Technology (IJETT)*, 16(8):382–385, 2014.

[27] Plastics International. Hardness Scale - Durometer Comparisons of Materials, 2015.

[28] Data Sheet. Power Digital MEMS Accelerometer. pages 1–32, 2012.

[29] Linear Technology. LTC3331 - Nanopower Buck-Boost DC/DC with Energy Harvesting Battery Life Extender. pages 1–32.

[30] S. Tornincasa, M. Repetto, E. Bonisoli, and F. Di Monaco. Energy harvester for vehicle tires: Nonlinear dynamics and experimental outcomes. *Journal of Intelligent Material Systems and Structures*, 23(1):3–13, 2012.

[31] L Wang and F-G Yuan. Structural Vibration Energy Harvesting by Magnetostrictive Materials (MsM). *4th China-Japan-US Symposium on Structural Control and Monitoring*, pages 1–8, 2006.

[32] Hugh D. Young and Roger A. Freedman. *University Physics.* Pearson, 12th edition, 2008.

[33] Qi Zhang, Amen Agbossou, Zhihua Feng, and Mathieu Cosnier. Solar micro-energy harvesting with pyroelectric effect and wind flow. *Sensors and Actuators, A: Physical*, 168(2):335–342, 2011.